BROADBAND AND LOW PROFILE ANTENNA FOR UHF BAND

N. Riauka, G. Hjipieris, J. C. Vardaxoglou
Antrum Ltd, Loughborough Innovation Centre,
Epinal Way, Loughborough, LE11 3EH
E-mail: yiannisv@antrum.co.uk

Abstract

The requirement of wideband and compact devices is ever increasing in most communication systems. In addition, recent increases in the transmission and reception of information have created a need for broadband and low profile antennas. This necessity is particularly challenging in designing Radio Frequency (RF) products that demand these features at low RF bands. There are numerous situations in which environmental considerations and application require the antenna to also be low-profile.

1. Introduction

This paper discus a study performed in a novel, broadband, low cost and low profile antenna in the UHF band. This has been achieved through numerical modelling, theoretical investigation and physical measurements. The dual side Printed dipole antenna (PDA) is used as a main radiating element. Also the use of the microstripe tapered balun and the parasitic elements increase the operation band of the antenna. The general PDA structure is shown in Figure 1. The main parts are: the tapered balun (A), the parallel strip transmission line, matching section (B), the driven element (C) and the parasitic elements (D).

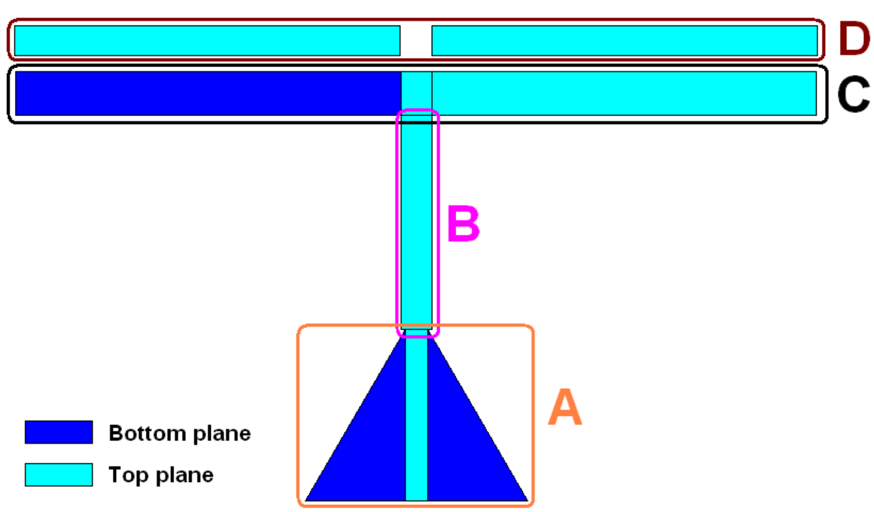

Figure 1 General PDA structure

The balun is created by using the microstrip line transformation to the parallel strip line as the balancing transition. The tapered baluns are frequently used as the balanced transmission line to feed various printed antennas [1, 2] or in microwaves mixers [3, 4]. The concept of using tapered balun was introduced by Duncan and Minerva in 1959 [4]. They used baluns to excite the wide band balanced aerials. The balun was designed as the impedance transformer from the unbalanced to balanced line, relied on a gradual change of the cross section of the transmission line. The linearly tapered transitions, used to perform a wide band operation, are reported in [5, 6].

The driven element is $\lambda_0/2$ dipole. Its radiation resistance is equal to 73Ω. In printed dipole antennas the increase in the width of the printed arms is identical to the increase in the radius of an equivalent wire dipole. This is a well known technique for the bandwidth widening of wire dipoles. However, the radiation efficiency might decrease by applying this technique [7, 8].

The radiation pattern, the gain and the return loss can be improved by introducing the parasitic element to the antenna structure. The parasitic element can be described as a radiating element not driven by a feed line but coupled to a directly fed radiator [9]. The use of parasitic elements in close proximity to the dipole arms has been proposed by Evtioushkine et al [10]. In this case the bandwidth was boosted from 39% to 56% by introducing the parasitic elements, suspended over a ground plane configuration [11].

2. PDA simulations

The PDA was simulated using CST MicroStripes software. The Structure of the PDA is shown in Figure 2.

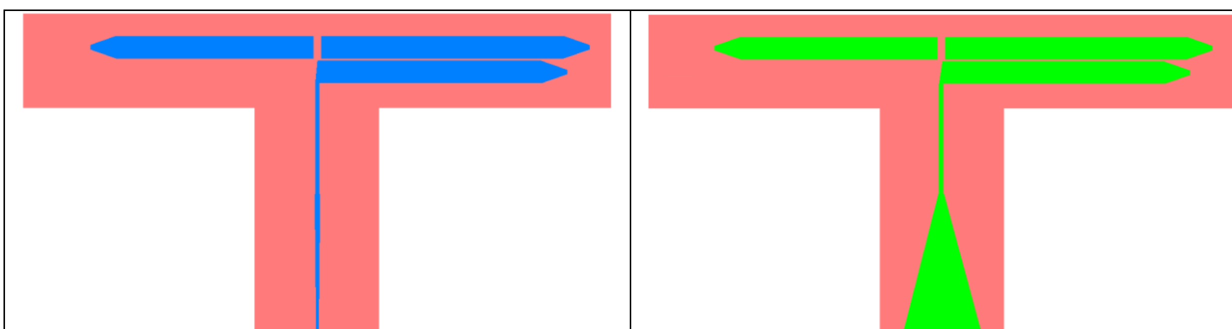

Top view	Bottom view

Figure 2 Structure of the PDA with tapered balun and parasitic elements

The PDA is optimised to work within 470MHz - 850MHz band. The return loss, the real (R_{in}) and the imaginary (X_{in}) parts of the input impedance and the antenna input impedance (Z_{char}) values are shown in Figure 3.

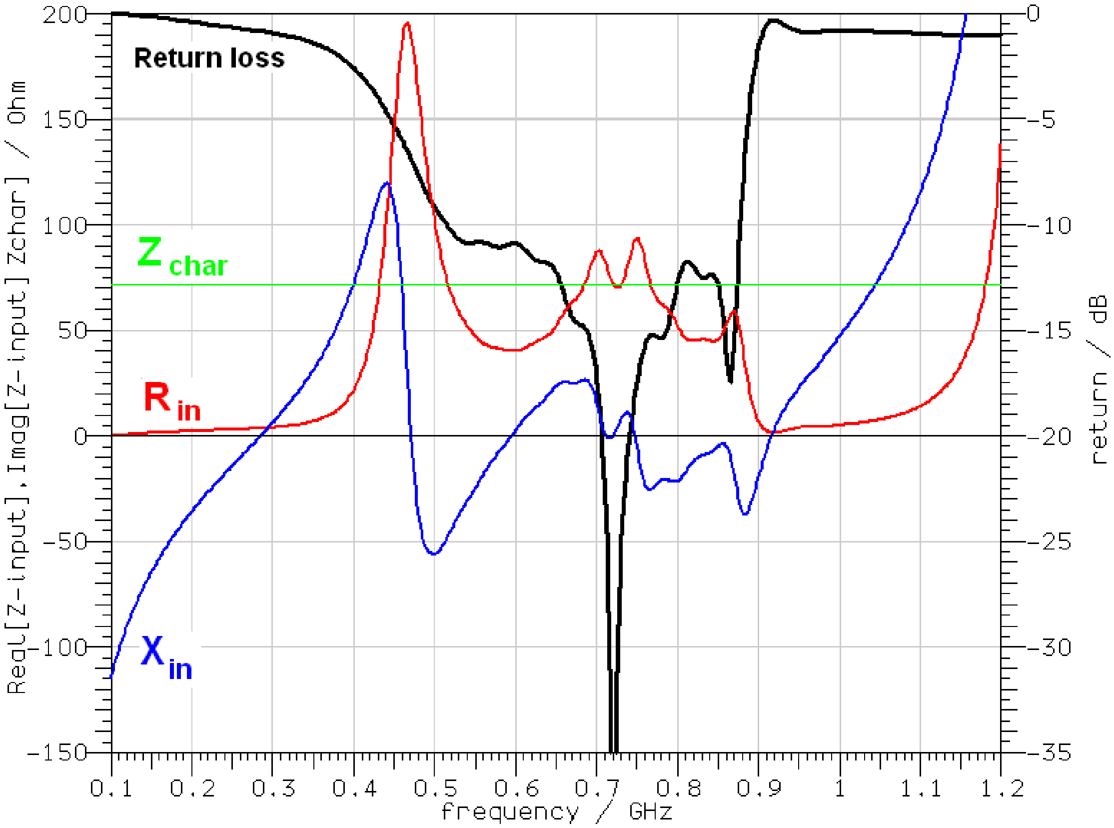

Figure 3 Simulated PDA results

The achieved bandwidth is 52.9%. The simulated antenna efficiency varies from 88% to 97.7%. The obtained PDA directivity and gain values are as high as 4.3dBi and 4.1dBi respectively.

The balun balancing phenomena can be proved by two criteria. Firstly, the surface current distribution must have the same value at symmetrical points of the input to the radiating element. Secondly, the direction of the surface current distribution at these points must be opposite.

The surface current distribution at each frequency (470MHz, 550MHz, 650MHz, 750MHz and 850MHz) is shown for two phases: when the surface current distribution is maximum and when it is equal or close to zero. The surface current distribution results for the first three frequencies (i.e. 470MHz. 550MHz and 650MHz) are represented in Figure 4. For other frequencies (i.e. 750MHz and 850MHz) the surface current distribution is shown in Figure 5.

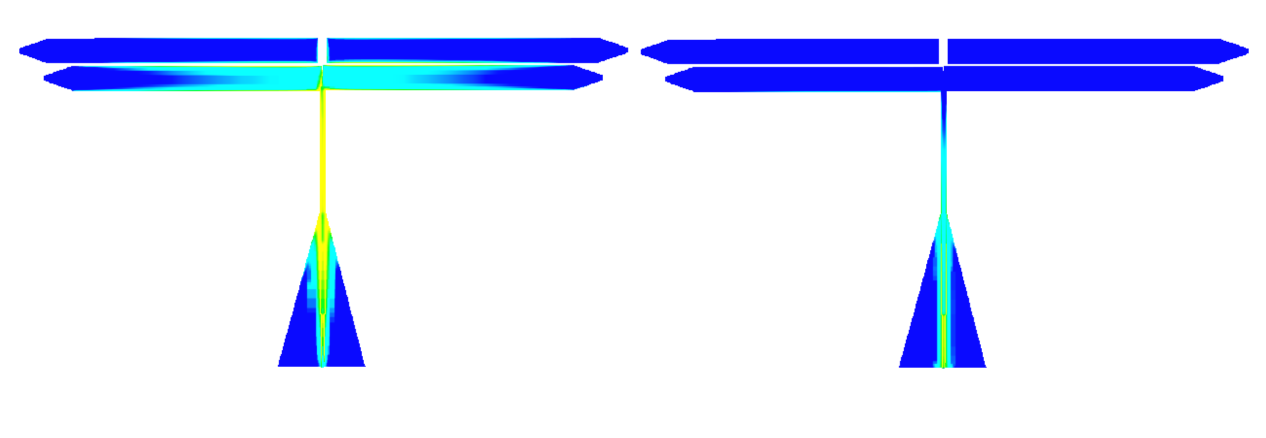

470 MHz ϕ=80°	470 MHz ϕ=170°

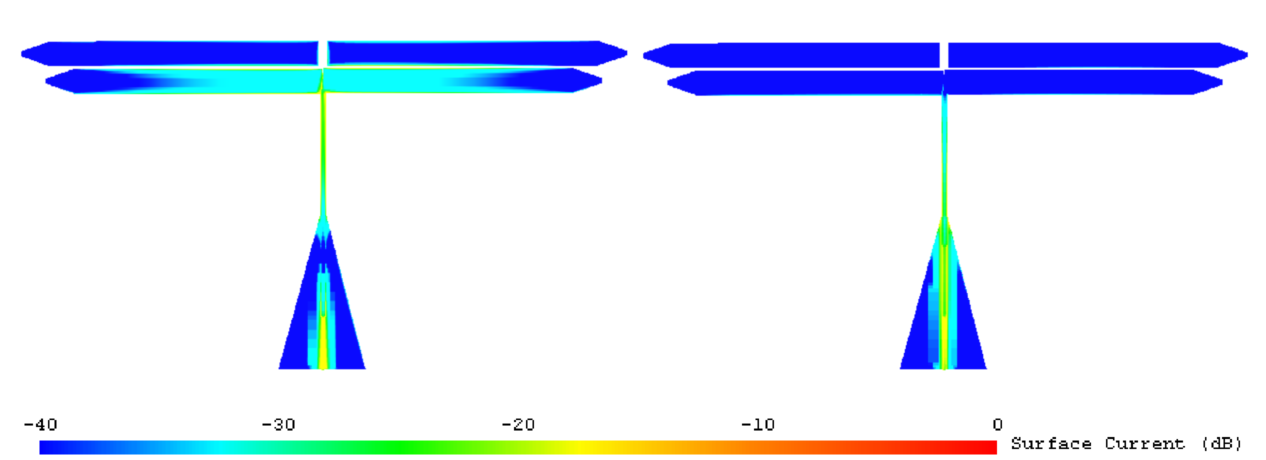

550 MHz ϕ=20°	550 MHz ϕ=110°

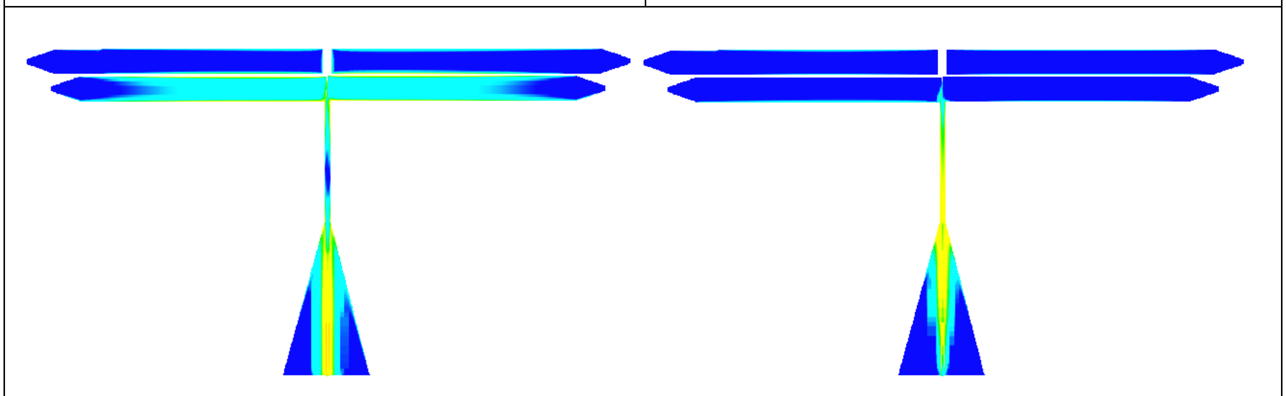

650 MHz ϕ=40°	650 MHz ϕ=130°

Figure 4 Simulated OPDAwP surface currents at 470MHz, 550MHz and 650MHz

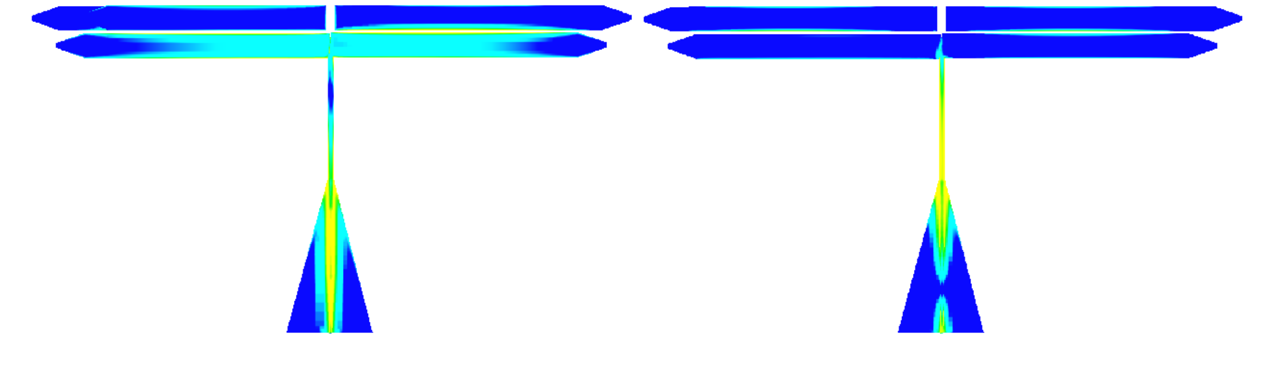

750 MHz ϕ=210°	750 MHz ϕ=300°

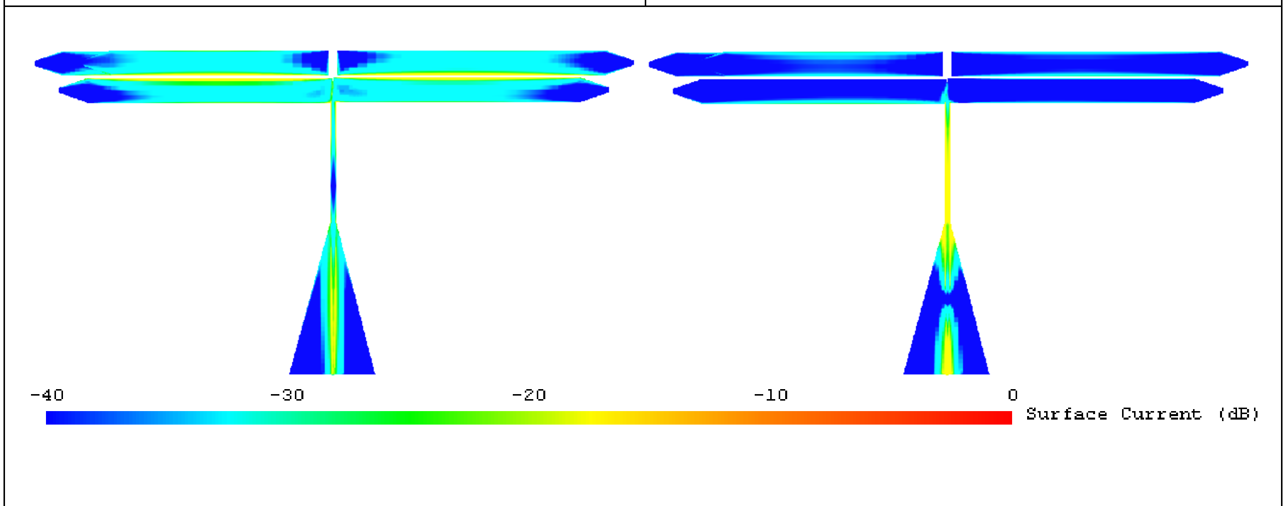

850 MHz ϕ=110°	850 MHz ϕ=200°

Figure 5 Simulated OPDAwP surface currents at 750MHz and 850MHz

Figure 6 illustrates the direction of the PDA surface currents at central frequency of 650MHz. It should be noted that their direction is the same at the symmetrical points of the PDA dipole, however at the parallel strip line these direction are opposite.

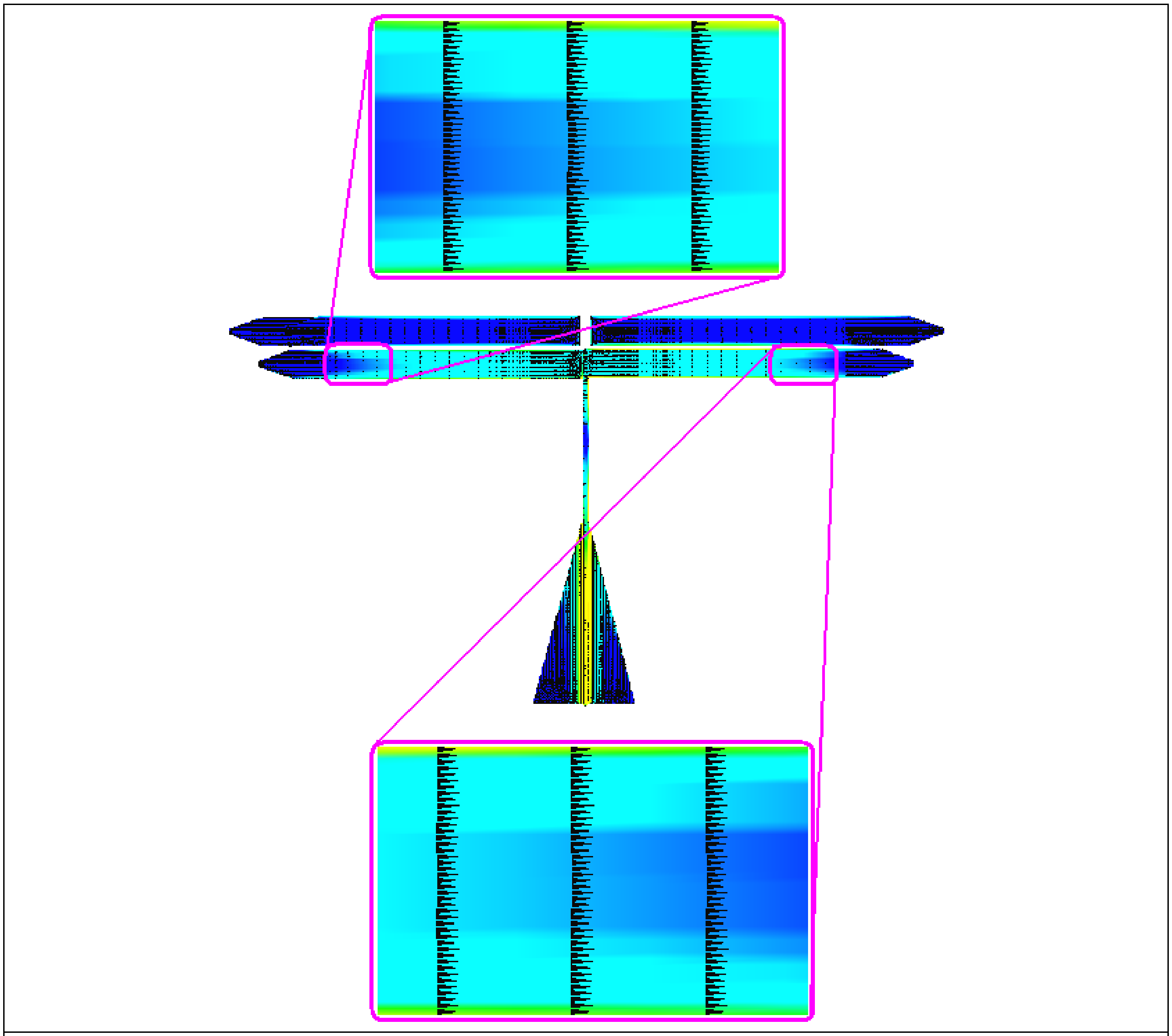

Figure 6 Simulated surface current directions of OPDAwP at 650MHz

The radiation patterns play an important role in describing any antenna operation. The E- plane and the H- plane, co-polar and x-polar radiation patters of the PDA are shown in Figure 7. The first four pictures illustrate the E-plane, the H-plane co-polar and x-polar 2D radiation patterns at following frequencies: 470MHz, 550MHz, 650MHz and 750MHz. They are similar to the ones stated in the theory for the $\lambda_0 / 2$ wire dipole. At the E-plane the PDA acquires the radiation patterns in a shape of the figure eight. At the H-plane it acquires the omnidirectional radiation patterns [7]. However, the patterns at 800MHz-850MHz are alternated by the parasitic element, coupled from the exited active element. The active element reflects the parasitic element radiation.

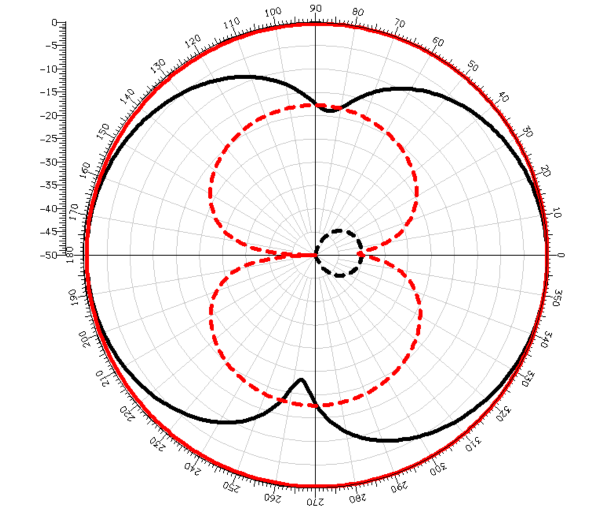

470 MHz

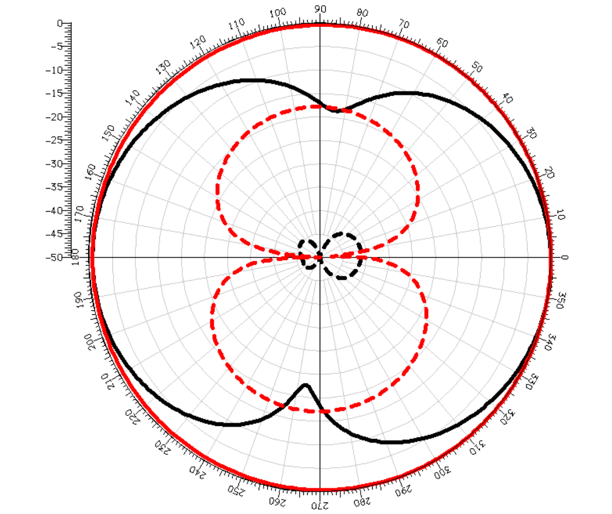

550 MHz

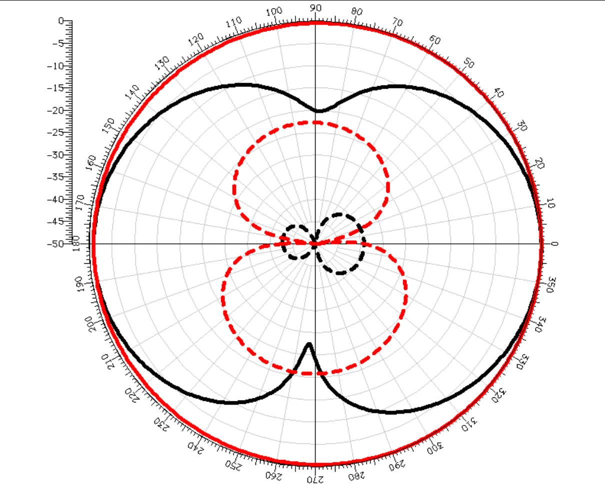

650 MHz

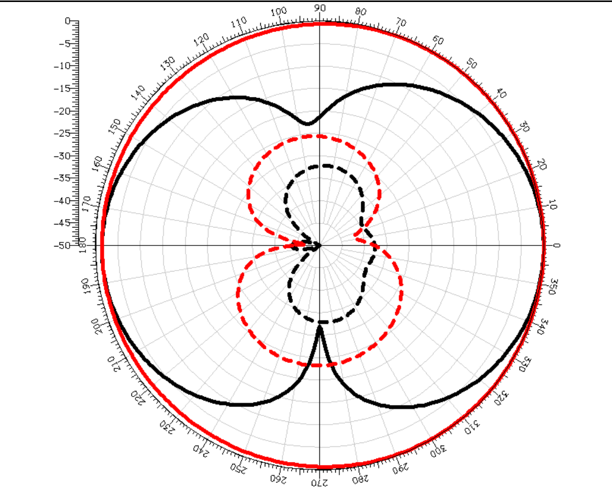

750 MHz

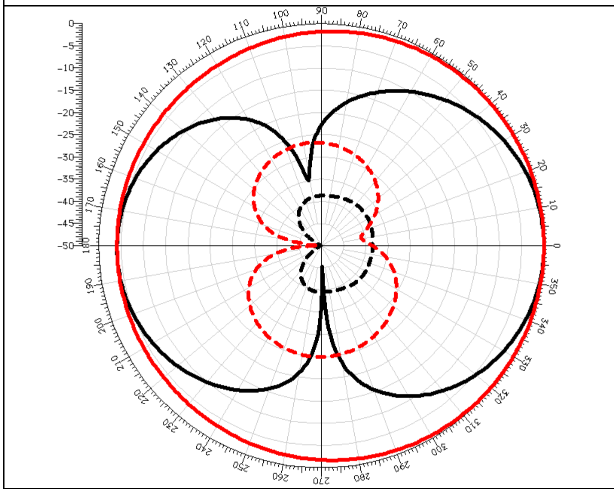

850 MHz

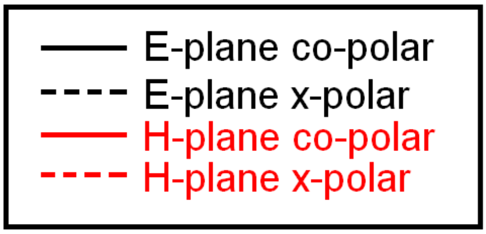

Figure 7 Simulated PDA radiation patterns

3. Manufactured PDA

The measurements were carried out by using the ANRITSU MS2026A portable vector network analyzer (VNA) [12] in the anechoic chamber. The VNA calibration was performed by using the 75Ω Rosenberger F-type socket calibration kit (model 74CK10A-170) [13]. The F - type female sockets of 75Ω were chosen to be used as connectors in these PDA prototypes. Also The FR4 substrate with the permittivity of 4.9 and the thickness of 1.52 was used in the manufacturing. The top and the bottom views of the manufactured PDA are shown in Figure 8.

	
PDA top view	PDA bottom view

Figure 8 Manufactured OPDAwP model compared to one pound coin

The measurement results are compared to the simulated ones in Figure 9.

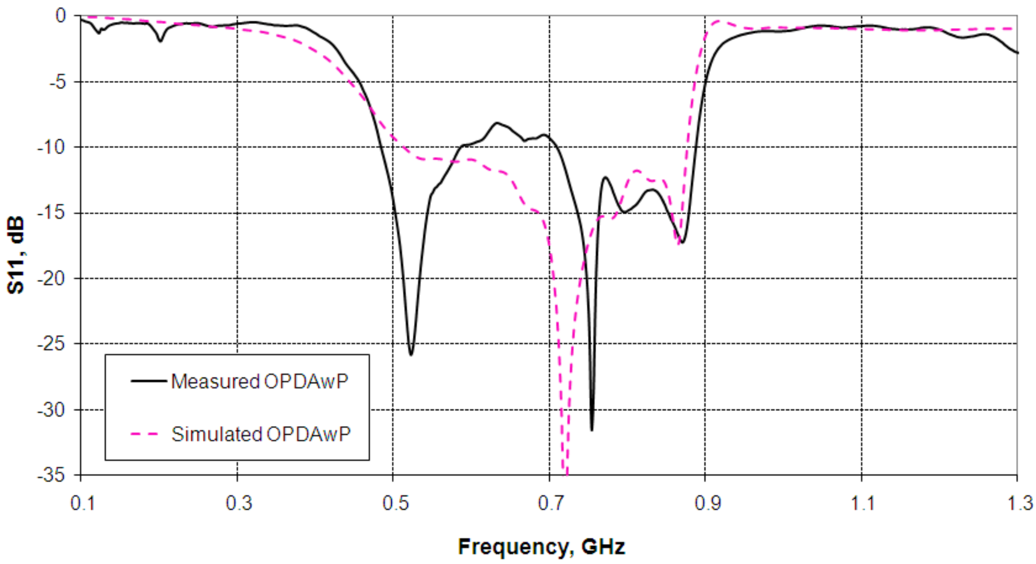

Figure 9 The simulation and measurement results of the PDA

The measured PDA bandwidth is equal to 56.8%, which is 3.9% larger than the simulated bandwidth. The minimum measured return loss value at 524MHz is -26 and at 756Hz is about -32dB.

4. Conclusions

The novel, balanced, broadband and the low cost antenna was developed. The printed dipole antenna structure was analysed and the main PDA parts explained. The measured PDA bandwidth was equal to 56.8%, which was 3.9% larger than the simulated bandwidth. The simulated antenna efficiency varied from 88% to 97.7%. The obtained PDA directivity and gain values were as high as 4.3dBi and 4.1dBi. Also to prove the broadband balancing phenomena, surface current distribution for the maximum and zero values was extracted at various

References:

[1] R. Garg, P. Bhartia, I. Bahl, and A. Ittipiboon "Microstrip Antenna Design Handbook", Norwood, MA: Artech House, 2001.

[2] N. Fourikis, N. Lioutas, and N. V. Shuley, "Parametric study of the co and x-polarization characteristics of tapered planar and antipodal slot antennas," Proc. Inst. Elect. Eng., pt. H, vol. 140, pp. 17–22, Feb.1993.

[3] M. A. Smith, K. J. Anderson, and A. M. Pavio, "Decade-band mixer covers 3.5 to 35 GHz," Microwave J., pp. 163–171, Feb. 1986.

[4] J.W. Duncan, V.P. Minerva: "100: 1 Bandwidth balun transformer", Proc. IRE, 1960, 48, pp. 156-164.

[5] B. Climer, "Analysis of suspended microstrip taper baluns," Proc. Inst. Elect. Eng., pt. H, vol. 135, pp. 65–69, Apr. 1988.

[6] S.G. Kim, K.Chang, "Ultra wide -Band Transitions and New Microwave Components Using Double-Sided Parallel-Strip Lines", IEEE transactions on Microwave theory and Techniques vol. 52 pp.2148-2152, September, 2004.

[7] C. A. Balanis "Antenna theory analysis and design" 2nd edition, New York, Wiley, 1997.

[8] A.W. Rudge, K.Milne, A.D. Olver, P.Knight "The handbook of antenna design", volumes1 and 2, Page Bros Ltd, Norfolk,1986.

[9] A.W. Rudge, K.Milne, A.D. Olver, P.Knight "The handbook of antenna design", volumes1 and 2, Page Bros Ltd, Norfolk,1986.

[10] G.A Evtioushkine, J.W Kim and K.S. Han "Very wideband printed dipole antenna array", Elelctron Lett 34 (1998), 2292-2293.

[11] T.G. Vasiliadis, E.G. Vaitsopoulos, and G.D. Sergiadis "A wideband printed dipole antenna with optimised tapered feeding balun for ISM and FWA bands" Microwave Opt Technol Lett 43 (2004), 437-441.

[12] Anritsu VNA Master MS2024A - MS2026A User's Guide, 2 November 2005, UK; Anritsu VNA Master MS2024A/MS2026A and MS2034A/MS2036A Programming Manual, 24 October 2006, UK.

[13] Rosenberger website: http://www.rfmw.com/rosenberger/?src=adwords&pid=241